

Single-Particle and Collective Motion for Proton-Rich Nuclei on the Astrophysical rp-Process Path

Yang Sun^(1,2), Jing-ye Zhang⁽¹⁾, Mike Guidry⁽¹⁾, Jie Meng⁽³⁾ and Soojae Im⁽³⁾

⁽¹⁾*Department of Physics and Astronomy, University of Tennessee, Knoxville, Tennessee 37996*

⁽²⁾*Department of Physics, Xuzhou Normal University, Xuzhou, Jiangsu 221009, P.R. China*

⁽³⁾*Nuclear Theory Laboratory, Department of Technical Physics, Peking University, Beijing 100871, P.R. China*
(December 2, 2024)

Based on available experimental data, a new set of Nilsson parameters is proposed for proton-rich nuclei with proton or neutron numbers $28 \leq N \leq 40$. The resulting single-particle spectra are compared with those from relativistic and non-relativistic mean field theories. Collective excitations in some even-even proton-rich nuclei on the rp-process path are investigated using the Projected Shell Model with the new Nilsson basis. It is found that the regular bands are sharply disturbed by band crossings involving $1g_{9/2}$ neutrons and protons. Physical quantities for exploring the nature of the band disturbance and the role of the $1g_{9/2}$ single-particle are predicted, which may be tested by new experiments with radioactive beams.

21.10.Pc, 21.10.Re, 21.60.Cs, 27.50.+e

Hydrogen can be burned explosively in a high-temperature ($\sim 10^8 - 10^9$ K) and high-density ($\sim 10^3 - 10^8$ g/cm³) environment such as novae or X-ray bursts [1]. Under such astrophysical conditions, hydrogen burning can transmute nuclei from the CNO region to much heavier nuclei on explosive time scales. Through radiative proton captures and β^+ decays (with a few (α, γ) and (α, p) reactions), the rapid proton capture or rp-process [2] can proceed along a path in the chart of nuclides close to the proton drip line.

In general, the quality and predictive power of all astrophysical models for energy generation as well as for nucleosynthesis depend crucially on the quality of input parameters. The path of the rp-process is a very complicated function of the physical conditions governing the explosion. Study of the rp-process requires nuclear physics inputs such as masses, lifetimes, proton capture cross sections and β -decay rates for unstable, proton-rich nuclei [3]. For nuclei beyond $Z = 32$ and $A = 64$, the β -decay half-lives of nuclei close to the proton drip line are especially important. However, for most of these nuclei no experimental data are available. Therefore, the ground-state β -decay rates as well as the decay rates from thermally populated excited states must be calculated.

For reactions occurring near the proton drip line, compound nuclei are formed at very low excitation energies and therefore at low level densities, which does not justify Hauser-Feshbach calculations. Thus, detailed nuclear structure information is required. One hopes that radioactive beams will provide us with the information eventually, but one has to rely on theoretical calculations at present. To obtain detailed nuclear structure, advanced shell model diagonalization methods, which can give explicitly spectroscopy and matrix elements for all kinds of nuclei (even-even, odd-A and odd-odd), are of particular importance. One example from recent studies [4] has demonstrated that large-scale shell model di-

agonalizations can significantly improve the theoretical Gamow-Teller distributions and spectra of nuclei in the mass range $A = 45 - 65$. Based on these results, the calculated electron capture rates for supernova environment are found to be significantly smaller than that currently assumed [5].

The Projected Shell Model (PSM) [6] is a shell model diagonalization carried out in a projected space determined by a deformed Nilsson-BCS basis. This kind of shell model truncation is highly efficient if the single-particle (SP) basis is realistic because the basis already contains many correlations [6]. It has been shown that the PSM can describe the spectra and electromagnetic transitions in normally deformed [6], superdeformed [7,8], and transitional nuclei [9]. One can further calculate the nuclear matrix elements for astrophysical processes such as direct capture and decay rates. One advantage of the PSM is that it can easily handle heavy, well-deformed nuclear systems. This can be important for the structure study of significantly deformed nuclei ($Z = 36 - 40$) on the rp-process path, for which the current large-scale shell model diagonalizations are not feasible.

As an initial step for a PSM study, a reliable Nilsson model calculation [10,11] is required to build the projected space. The Nilsson model has been used widely in nuclear structure studies. Its “standard” set of parameters κ and μ [11] has been quite successful in describing the SP structure for stable nuclei across the whole chart of nuclides. However, previous work has shown that the standard Nilsson SP energies are no longer realistic for the neutron-rich region [12]. Thus, an adjustment of these parameters is necessary for unstable nuclei.

Experimental SP states above the $N = 28$ shell closure can be read from the low-lying states of ^{57}Ni [13] and ^{57}Cu [14], the nearest neighbors of the doubly magic nucleus ^{56}Ni . These low-lying $2p_{3/2}$, $1f_{5/2}$ and $2p_{1/2}$ states are well characterized as pure SP levels [15]. According

to Ref. [16], the neutron $1g_{9/2}$ state lies 3.7 MeV above the $2p_{3/2}$ orbital. For the proton $1g_{9/2}$ state, the best experimental information available is the observation of a low-lying $\frac{9}{2}^+$ level in ^{59}Cu [17] and ^{61}Cu [18]. We may reasonably assume this level to be the $1g_{9/2}$ state because of its unique parity. Taking the deformation of $^{59,61}\text{Cu}$ [19] into account, the position of the proton SP $1g_{9/2}$ state can be estimated to lie 3.15 MeV above the $2p_{3/2}$ orbital.

When compared with these data, the standard Nilsson parameterization [11] produces energies for the $1f_{5/2}$, $2p_{1/2}$ and $1g_{9/2}$ orbits that are too high relative to the $2p_{3/2}$ orbit. To reproduce experimental data, one must reduce the strength of the spin-orbit interaction κ for $N = 3$ substantially from the standard value because of the observed smaller separation between $2p_{1/2}$ and $2p_{3/2}$ levels, and because of the position of $1f_{5/2}$ orbital. On the other hand, the pair of g -orbitals require a larger value of κ for $N = 4$ to position the $1g_{9/2}$ orbital properly. In Table I, we summarize the adjusted proton and neutron κ and μ parameters for the $N = 3$ and 4 shells that best reproduce the available data. The standard values for the $N = 2$ shell are also displayed without modification.

Relativistic Mean Field (RMF) theory [20] with non-linear self-interactions between mesons has been used in many studies of low-energy phenomena in nuclear structure. It has been extended recently to allow coupling between bound states and the continuum by the pairing force [21]. In the RMF theory, the spin-orbit interaction arises naturally as a result of the Dirac structure of the nucleons. As discussed above, the spin-orbit interaction is one of the important factors to give a correct SP energies. Thus, it is relevant to consider the relation of the SP Nilsson spectrum to that of the RMF. Here, two typical interactions, NL1 and NL3, are used. The latter interaction is suitable for nuclei away from the β -stability valley [22]. For comparison, SP energies from the non-relativistic Hartree-Fock calculations with the Skyrme interactions (SHF) (see Ref. [23] and references therein) are also presented.

In Fig. 1, theoretical SP states (from the new and the standard [10,11] Nilsson parameterizations, from SHF with SkM* and SIII forces, and from RMF with NL1 and NL3 interactions) are compared with data. It is obvious that the standard Nilsson parameters produce a large spin-orbital splitting for $2p_{1/2}$ and $2p_{3/2}$, and high excitation energy for $1f_{5/2}$ while the new set of parameters reduces these values. The SHF and RMF calculate the SP states for ^{56}Ni . Without specific parameter adjustment for this mass region, SP levels of the RMF with NL3 for the p and f orbitals are found to be reasonably close to the data. However, the SHF with the SkM* force produces rather wrong positions for all levels considered. In all the SHF and RMF calculations, the positions of

both neutron and proton $1g_{9/2}$ orbital are much too high.

The new Nilsson parameters should represent a better basis from which more sophisticated wave functions can be constructed. Therefore, we may test the new parameters by employing them in calculations that have a direct connection with measured collective spectra. For such a test, we shall employ the PSM to calculate the yrast bands of some even-even nuclei for which limited data are available for comparison: $^{62,66}\text{Zn}$ and $^{64,66}\text{Ge}$. These nuclei lie on the rp-process path, and ^{64}Ge is a waiting point nucleus [3] that was used as a test case for the recently proposed Quantum Monte Carlo Diagonalization Method (QMCD) [24]. As we shall see, the new Nilsson SP states discussed above can modify substantially the level spacings, position and sharpness of band crossing, and electromagnetic transition properties along a level sequence.

In PSM calculations of the collective states relevant here, the projected multi-quasiparticle (qp) space consists of 0-, 2-qp and 4-qp states for even-even nuclei, typically with a dimension of 50. This small shell model basis is sufficiently rich that the quality of the calculations is comparable to those from large-scale shell model diagonalizations [25]. For the SP basis we use three full major shells: $N = 2, 3$, and 4 for both neutrons and protons. This is the same size SP basis as employed in Ref. [8]. The deformation parameters are taken from Ref. [19] as follows: $\varepsilon_2 = 0.167$ and $\varepsilon_4 = -0.020$ for ^{60}Zn , $\varepsilon_2 = 0.192$ and $\varepsilon_4 = 0.013$ for ^{62}Zn , $\varepsilon_2 = 0.200$ and $\varepsilon_4 = 0.047$ for ^{64}Ge , and $\varepsilon_2 = 0.208$ and $\varepsilon_4 = 0.067$ for ^{66}Ge . The Hamiltonian is the usual quadrupole-quadrupole plus monopole pairing form, with quadrupole pairing included [6]. The strength of the quadrupole-quadrupole force in the Hamiltonian is determined self-consistently, and the monopole pairing strength is the same as that in Ref. [8]. For the four nuclei calculated in this paper, the ratio of quadrupole pairing to monopole pairing strength is fixed at 0.30.

In Fig. 2, yrast band (lowest energy state for given spin) transitional energies $E(I) - E(I - 2)$ are plotted as a function of spin I . It is obvious that the calculations employing the new set of Nilsson parameters reproduce the data very well, while those with the standard set of Nilsson parameters determined in the stability valley are in poorer agreement. In all the four nuclei, the standard set of Nilsson parameters gives too large level spacings for low-spin states, leading to the excitation energies that are too high. Note that the two calculations are performed with the same conditions except for different SP bases. It is the change in SP states that gives rise to the different results for the yrast spectrum.

Following the yrast band in a nucleus in Fig. 2, one observes a sudden drop in $E(I) - E(I - 2)$ at spin $I = 8$ or 10, which corresponds to a backbending in the moment of inertia for the system [6]. For these $N \sim Z$ nuclei, neutron and proton Fermi levels are surrounded by or-

bits with the same Nilsson quantum numbers. Therefore, bands built on the neutron and proton $1g_{9/2}$ intruder orbits can have a similar probability to be the first that crosses the ground band and becomes a major part of the yrast band. From analysis of the wave functions, we find that the sudden drop is caused by such band crossings. The crossing bands have either 2-neutron $1g_{9/2}$ or 2-proton $1g_{9/2}$ configurations.

Effects of the band crossing can be seen more clearly by looking at the reduced transition rates $B(E2)$. In the $B(E2)$ calculations, the effective charges are 0.5e for neutrons and 1.5e for protons, which are the same as those used in previous work and in other shell models [25]. Our results for the first two transitions in ^{64}Ge are close to those obtained in QMCD [24]. We emphasize that employment of different effective charges can modify the absolute values, but the essential spin dependence is determined by the wave functions. In Fig. 3a, the sudden drop in the $B(E2)$ values at spin $I = 8 - 10$ is consequence of band crossings discussed above. The drop indicates that the transition rate is sharply reduced by the structure change in the yrast band wave function. It is interesting to point out that our prediction for the crossings occurs exactly at the excited states where energy spectra measured to date have terminated (see Fig. 2). Thus the band crossing predictions may explain why the experimental measurements have not seen higher spin states.

The gyromagnetic factor (g-factor) is the quantity most sensitive to the SP components in wave functions as well as to their interplay with collective degrees of freedom. Because of the intrinsically opposite signs of the neutron and proton g_s , a study of g-factors enables determination of the microscopic structure for underlying states. For example, variation of g-factors often is a clear indicator for a SP component that strongly influences the total wave function. In the calculations we use for g_l the free values and for g_s the free values damped by the usual 0.75 factor. The results are presented in Fig. 3b.

Rather similar behavior is seen for all the four nuclei for spin states before band crossing: The g-factor values are close to the collective value of Z/A and tend to increase slightly as a function of spin. However, the pattern diverges at band crossing. The g-factors of the two $N = Z$ nuclei (^{60}Zn and ^{64}Ge) jump suddenly to a value near 1, while those of the two $N = Z + 2$ nuclei (^{62}Zn and ^{66}Ge) drop to zero. By analysis of the wave functions, we have found that this interesting behavior is determined by whether the proton or neutron $1g_{9/2}$ 2-qp states is lower in energy after band crossing. For $N = Z$ nuclei, proton $1g_{9/2}$ 2-qp states dominate the wave functions after band crossing, thus increasing the g-factors. For $N = Z + 2$ nuclei, neutron $1g_{9/2}$ 2-qp states become lower due to different neutron shell fillings, leading to very low values of the g-factors.

Similar band crossing pictures should be common for this mass region, and may also be seen in the neighbor-

ing odd-A and odd-odd nuclei. Successful measurement of the $B(E2)$ values and g-factors before and after band crossing would test our PSM predictions as well as the Nilsson SP states proposed in this paper. We hope that recently developed techniques [27] in combination with radioactive beams can permit such measurements.

In summary, a new set of Nilsson parameters is proposed for proton-rich nuclei beyond ^{56}Ni . This new set of parameters can be employed for proton-rich nuclei with proton and number numbers $N = 28 - 40$. Our results suggest that improved SP structures may be necessary for this mass region in SHF and RMF theories. Available data for yrast bands in some even-even nuclei on the rp-process path are well reproduced by PSM calculations with the new set of Nilsson states as a basis. Distinct signatures for the role of neutron and proton $1g_{9/2}$ orbitals are seen in the band crossings and the electromagnetic transitions along the yrast bands. We conclude that precise positions of the $1g_{9/2}$ SP orbitals are very important for any realistic calculations. Predictions of the present paper concerning the $1g_{9/2}$ band crossings, $B(E2)$ values, and the remarkably different behaviors of the g-factors at the crossings await future experimental tests.

Research at the University of Tennessee is supported by the U. S. Department of Energy through Contract No. DE-FG05-96ER40983. This work was partially sponsored by the National Science Foundation of China under Project No. 19847002 and 19935030, and by SRF for ROCS, SEM, China.

-
- [1] A.E. Champagne and M. Wiescher, *Annu. Rev. Nucl. Part. Sci.* **42**, 39 (1992).
 - [2] R.K. Wallace and S.E. Woosley, *ApJS* **45**, 389 (1981).
 - [3] H. Schatz *et al.*, *Phys. Rep.* **294**, 167 (1998).
 - [4] E. Caurier, K. Langanke, G. Martinez-Pinedo and F. Nowacki, *Nucl. Phys.* **A653**, 439 (1999).
 - [5] K. Langanke and G. Martinez-Pinedo, preprint (nucl-th/0001018).
 - [6] K. Hara and Y. Sun, *Int. J. Mod. Phys.* **E4**, 637 (1995).
 - [7] Y. Sun, J.-y. Zhang and M. Guidry, *Phys. Rev. Lett.* **78**, 2321 (1997).
 - [8] Y. Sun, J.-y. Zhang, M. Guidry and C.-L. Wu, *Phys. Rev. Lett.* **83**, 686 (1999).
 - [9] J.-y. Zhang, Y. Sun, M. Guidry and D.H. Feng, *Phys. Rev.* **C52**, R2330 (1995); J.A. Sheikh and K. Hara, *Phys. Rev. Lett.* **82** 3968 (1999).
 - [10] S.G. Nilsson *et al.*, *Nucl. Phys.* **A131**, 1 (1969).
 - [11] T. Bengtsson and I. Ragnarsson, *Nucl. Phys.* **A436**, 14 (1985).
 - [12] J.-y. Zhang, Y. Sun, M. Guidry, L.L. Riedinger and G.A. Lalazissis, *Phys. Rev.* **C58**, R2663 (1998).
 - [13] M.R. Bhat, *Nucl. Data Sheets* **67**, 195 (1992).
 - [14] X.G. Zhou *et al.*, *Phys. Rev.* **C53**, 982 (1996).

- [15] K.E. Rehm *et al.*, Phys. Rev. Lett. **80**, 676 (1998).
- [16] D. Rudolph *et al.*, Eur. Phys. J. **A6**, 377 (1999).
- [17] R.B. Firestone *et al.*, *Table of Isotopes*, 8th edition (John Wiley & Sons, Inc., 1996).
- [18] S.M. Vincent *et al.*, Phys. Rev. **C60**, 064308 (1999).
- [19] P. Möller *et al.*, Atom. Data and Nucl. Data Tables **59**, 185 (1995).
- [20] P. Ring, Prog. Part. Nucl. Phys. **37**, 193 (1996).
- [21] J. Meng, Nucl. Phys. **A635**, 3 (1998).
- [22] G.A. Lalazissis, D. Vretenar and P. Ring, Phys. Rev. **C57**, 2294 (1998).
- [23] S. Im and J. Meng, Phys. Rev. **C**, in press.
- [24] M. Honma, T. Mizusaki and T. Otsuka, Phys. Rev. Lett. **77**, 3315 (1996).
- [25] K. Hara, Y. Sun and T. Mizusaki, Phys. Rev. Lett. **83**, 1922 (1999).
- [26] G. de Angelis *et al.*, Nucl. Phys. **A630**, 426c (1998).
- [27] R. Ernst *et al.*, Phys. Rev. Lett. **84**, 416 (2000).

FIG. 1. SP states for neutrons and protons. Experiment and calculations from Nilsson model with new parameter set, from the standard set, from SHF with SkM* and SIII forces, and from RMF with NL1 and NL3 parameterizations.

FIG. 2. Transition energies $E(I) - E(I-2)$ along the yrast band in ^{60}Zn , ^{62}Zn , ^{64}Ge and ^{66}Ge from experimental data [17,26] (filled triangles) and PSM calculations with the new set of Nilsson parameters (open circles), and with the standard Nilsson parameters (open squares).

FIG. 3. $B(E2)$ (in unit of e^2b^2) and g-factors in ^{60}Zn , ^{62}Zn , ^{64}Ge and ^{66}Ge from PSM calculations with the new set of Nilsson parameters.

TABLE I. Nilsson parameters κ and μ for the major shells $N = 2, 3$ and 4.

N	κ_p	new κ_p	μ_p	new μ_p	κ_n	new κ_n	μ_n	new μ_n
2	0.105		0.0		0.105		0.0	
3	0.090	0.039	0.300	0.222	0.090	0.035	0.250	0.293
4	0.065	0.087	0.570		0.070	0.097	0.390	

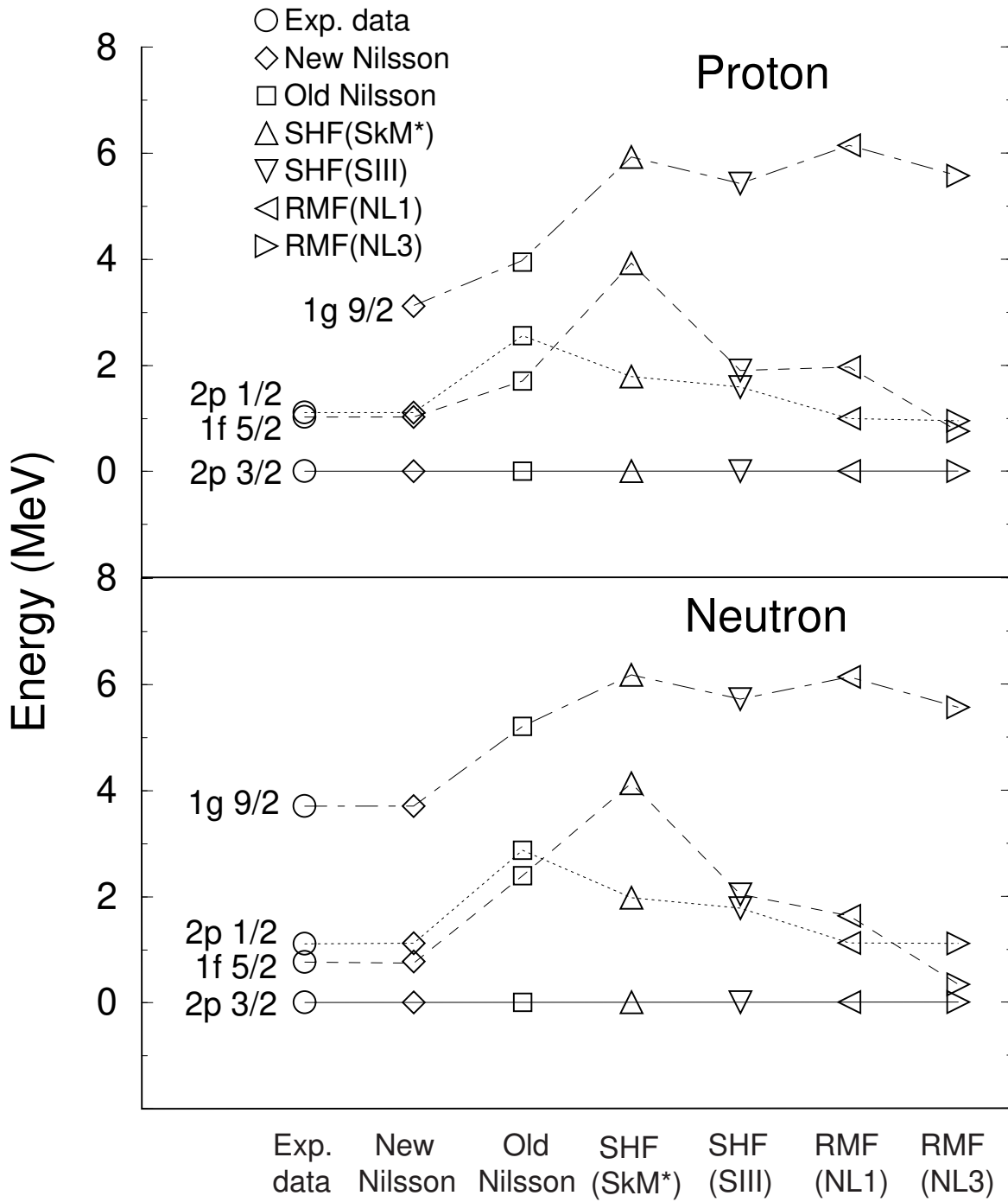
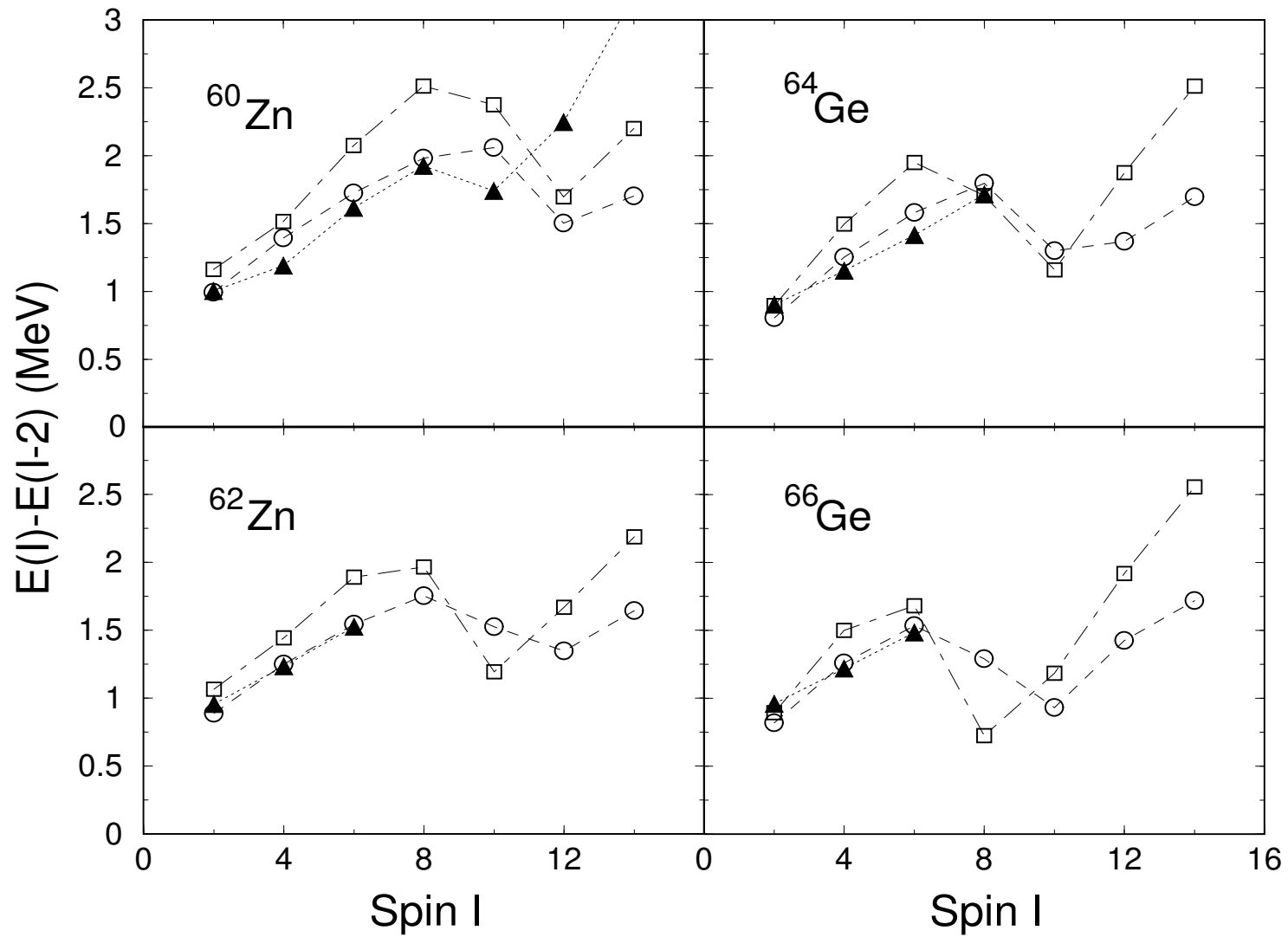


Fig. 1 Sun, Zhang, Guidry, Meng and Im

Fig. 2 Sun, Zhang, Guidry, Meng and Im



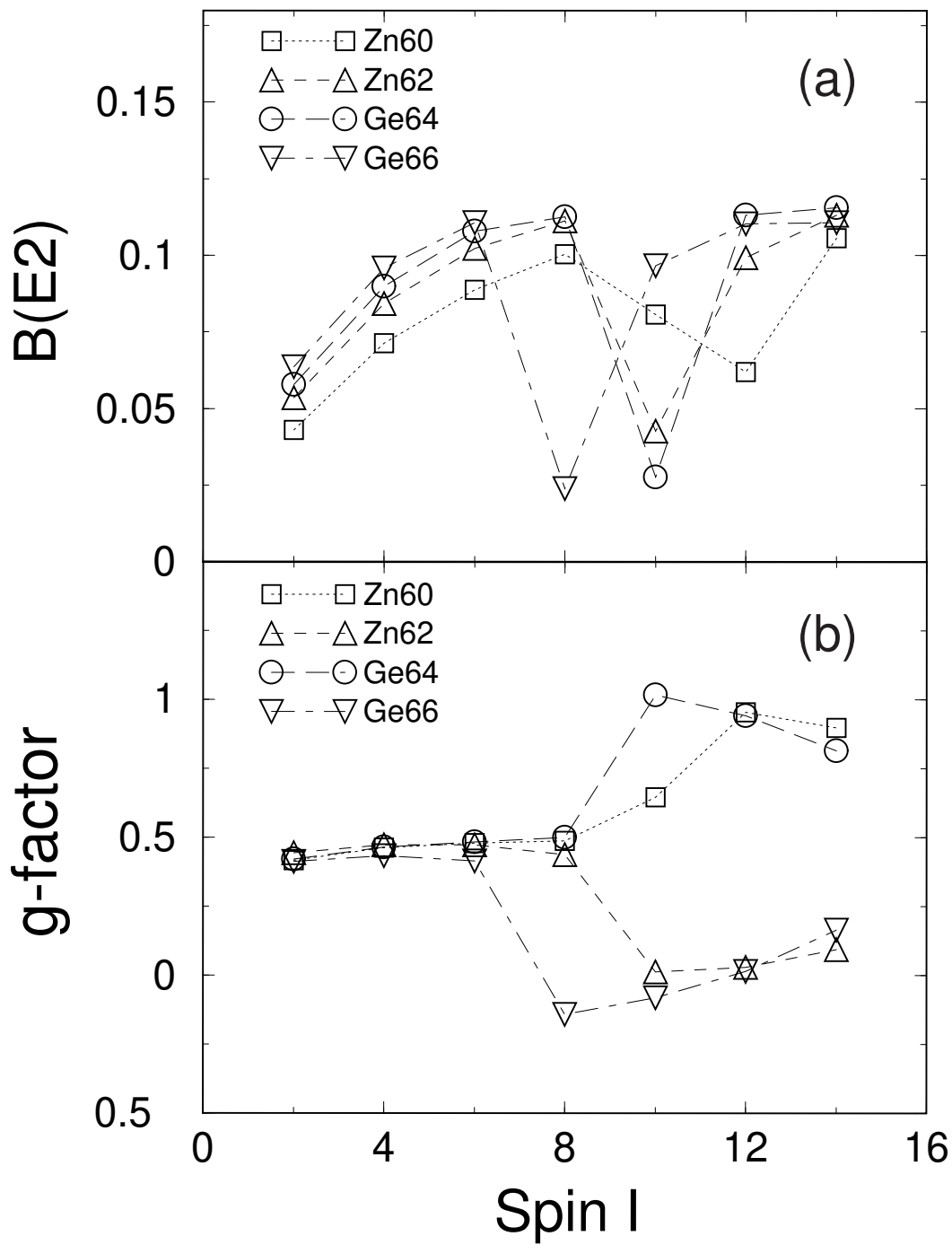


Fig. 3 Sun, Zhang, Guidry, Meng and Im